

Compounding of Nanocomposites by Thermokinetic Mixing

T. G. Gopakumar, D. J. Y. S. Pagé

Department of Chemistry and Chemical Engineering, Royal Military College of Canada, Kingston, Ontario K7K 7B4, Canada

Received 8 March 2004; accepted 2 September 2004

DOI 10.1002/app.21597

Published online in Wiley InterScience (www.interscience.wiley.com).

ABSTRACT: Nanocomposites have been prepared by melt mixing poly(propylene) (PP) and different levels of a premixed montmorillonite-organoclay masterbatch (PP/clay concentrate). Melt mixing was achieved using a Gelimat, a high-speed thermokinetic mixer. The Gelimat system is designed to handle difficult compounding and dispersion applications and can achieve mixing, heating, and compounding of products within a minute. Therefore, the thermal history of the compounded polymer is short, which limits degradation. The structure and properties of the nanocomposites prepared with a Gelimat were compared to ones prepared with a twin-screw extruder. The structure and

properties of PP/clay nanocomposites were compared by TEM, X-ray diffraction, mechanical testing, and rheological analysis. Results indicate that a better dispersion of the clay can be achieved by thermokinetic mixing when compared to extrusion, resulting in better mechanical properties. Calculations, based on simplifying assumptions, showed that the shear rates generated in a Gelimat are at least one order higher than those generally generated in an extruder. © 2005 Wiley Periodicals, Inc. *J Appl Polym Sci* 96: 1557–1563, 2005

Key words: compounding; nanocomposites; poly(propylene); clay

INTRODUCTION

Development of polymer nanocomposites, by dispersing nanoscopic fillers in commodity resins, is one of the latest evolutionary steps in polymer technology.^{1,2} Polymer nanocomposites exhibits superior mechanical properties, reduced gas permeability, improved solvent resistance, and enhanced conductivity. The enhanced reinforcement is a consequence of the much greater surface-to-volume ratio of these high-aspect-ratio fillers. These materials can be used to fabricate strong, lightweight, and durable composites for use in the automotive and aerospace industries. Nanofillers usually used so far are clay, alumina, nanotubes, gold, silver, and graphite.¹ Preparation and characterization of polymer nanocomposite based on polypropylene and montmorillonite type clay has been extensively reported.^{3–7} Interest in polyolefin nanocomposites has emerged due to their promise of improved performance in packaging and engineering applications. Chemical modification of these resins, in particular the grafting of pendant anhydride groups, has been used successfully to overcome problems associated with poor phase adhesion in polyolefin/clay systems.^{3,4}

The preparation of nanocomposites requires extensive delamination of the layered filler structure and complete dispersal of the resulting platelets throughout the polymer matrix.

Extrusion is the technique mostly used for melt processing polymers on an industrial scale. An extruder melts, mixes, and compresses polymers by screw action. One of the challenges with extruders is the difficulty in optimizing the performance of the above three functions effectively. Time for melting and mixing polymers and additives in an extruder requires several minutes, resulting in a potential thermal degradation of the polymers. The Gelimat system is specifically designed to handle difficult compounding and dispersion applications by completely heating, mixing, and compounding products within a few minutes. Therefore, the thermal history of the compounded polymer is short, which can limit degradation. The Gelimat has been used for processing polymers and additives.^{8–12} Busigin et al.⁸ used a Gelimat to compound mica with poly(propylene) (PP) and found that it can delaminate and disperse mica platelets in the polymer matrix. Baker et al.⁹ successfully used a Gelimat for dispersing pigments in polyethylene. Frenken et al.¹⁰ and Lyons and Baker¹¹ developed energy transfer models for polymer processing in a Gelimat. More recently, the authors studied the structure and properties of PP/graphite nanocomposites produced with a Gelimat.¹²

Correspondence to: D. J. Y. S. Pagé (page-d@rmc.ca).

Contract grant sponsor: Natural Sciences and Engineering Research Council of Canada.

The objective of this work is to produce PP/clay nanocomposites by exploiting the special features of a thermokinetic mixer like the Gelimat and to compare the structure and properties of these materials with nanocomposites prepared with a twin-screw extruder.

EXPERIMENTAL

Materials

Poly(propylene) (PP MFI = 4, Pro-fax 6325 Basell Chemicals) and graft-modified PP containing approximately 1 wt % of maleic anhydride (PP-g-MA, Polybond 3200 from Uniroyal) were used without purification. An organoclay (I.44PA) and its masterbatch (C.44PA) were supplied by Nanocor, Inc. (Arlington Heights, IL). TGA analysis showed that C.44PA contains 43% organoclay and 57% PP. The amount and type of the PP-g-MA compatibilizer used were not disclosed by the company.

Compounding

Nanocomposites containing 3 and 5 wt % organoclay were compounded by mixing the masterbatch (C.44PA) with the PP homopolymer. One series was produced using a Werner and Pfleiderer Gelimat 1-S thermokinetic mixer. The Gelimat was operated with at shaft speed of 2000 rpm (13.8 m/s at the tip of the blade) until the material reached 190°C. All batches were prepared with an identical load of 250 g, a speed of 2000 rpm, and a consolidation time of 90 s. The resulting mixing time in the melt state was 20–30 s. Another series of nanocomposites was produced using a twin-screw corotating intermeshing extruder, Model ZSK-30 by Werner and Pfleiderer, with a standard compounding configuration. The extruder was equipped with seven heating zones. Temperatures along the barrel ranged from 160°C for zone 1 (hopper) to 220°C for zone 7 (die). The screw speed was 100 rpm and the mass flow rate was 2 kg/h, corresponding to 10 min of mixing time in the melt state. Extruded strands were immersed in a trough containing cold water.

Characterization

The extent of clay exfoliation in the composites was determined by X-ray diffraction (XRD) using a Scintag XGEN 4000 diffractometer (Cu $K\alpha$ radiation $\lambda = 1.5406 \text{ \AA}$, generator voltage = 45 kV, current = 40 μA).

Clay dispersion and exfoliation was also determined by transmission electron microscopy (TEM). Thin sections (70 nm) were cut on a Leica Ultracut at -100°C and mounted on carbon-coated copper grids. The samples were viewed in a FEI Tecnai 20 transmis-

sion electron microscope at 200 kV. Images were collected on a Gatan Dualview digital camera.

Rheological characterization was performed from disks 25 mm in diameter and 2 mm in thickness that were prepared by compression molding at 190°C. The elastic modulus (G'), loss modulus (G''), and complex viscosity (η^*) were measured using a Reologica ViscoTech instrument as a function of the angular frequency (ω) from 0.04 to 188.50 rad/s. The rheometer was operated at $170 \pm 0.1^\circ\text{C}$ in the oscillatory mode with parallel plate fixtures 20 mm in diameter and at a gap of 1.5 mm. All measurements were carried out under nitrogen to limit polymer degradation or moisture absorption. Strain sweeps were performed to verify that the measurements were within the linear viscoelastic regime. Three measurements for each composite composition were performed.

Test specimens for tensile measurements were processed by injection molding. Strain at yield, tensile strength, and modulus were measured at a crosshead speed of 5 mm/min with an Instron 4206 extensometer in accordance with ASTM D638.

RESULTS AND DISCUSSION

Thermokinetic mixing

In a Gelimat, blades on a high-speed shaft accelerate the particles and impart them high kinetic energy, which is converted to thermal energy when they hit the chamber wall.⁹ The compounding time depends on the charge size, the rotor speed, and the properties of the material.¹⁰ To study the thermokinetic mixing of PP/clay-based nanocomposites, pure and filled PP were compounded. Figure 1 shows typical runs with current in amperes as a function of compounding time in seconds for pure PP, PP/organoclay, and PP/organoclay in the presence of a PP-g-MA compatibilizer. The current in amperes, used by the Gelimat, relates to the energy required for melting the polymer and mixing it with the additives. The compounding time can be divided in two segments, an induction time ($t_{\text{induction}}$), where solid particles collide and develop heat through friction, and a mixing time (t_{mix}), where the polymer melts and is mixed with the reinforcement and the additives. The energy required for compounding increases in the presence of PP-g-MA, as indicated by the increase in current. This is attributed to the higher viscosity resulting from the chemical interactions between PP-g-MA and hydroxyl groups present on the clay phase³ and to the energy required to exfoliate the clay.

X-ray diffraction

Figure 2 shows the XRD patterns of the nanocomposites (5 wt % organoclay) compounded from C.44PA

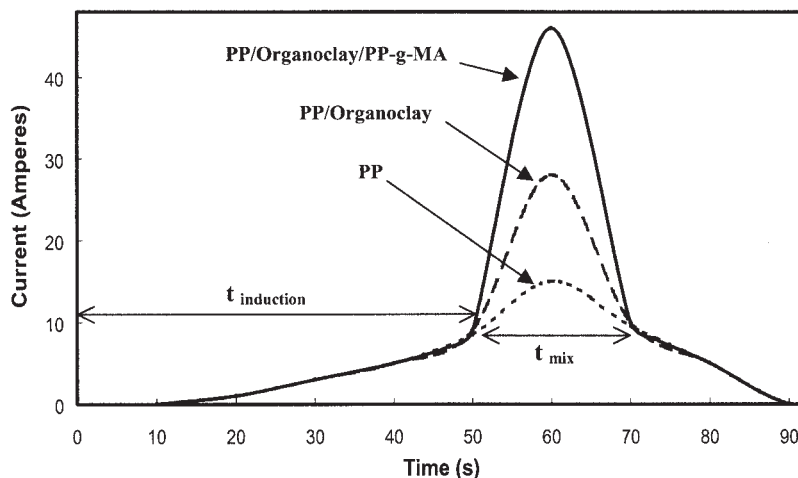


Figure 1 Gelimat mixing run for (.....) PP, (—), PP/5 wt % organoclay, and (—) PP/5 wt % organoclay/PP-g-MA compatibilizer.

and PP using the extruder and the Gelimat. For C.44 PA, the organoclay masterbatch, the peak at $2\theta = 3.44$ (25 \AA) indicates that clay platelets are not intercalated with PP. For the extruded nanocomposite with 5 wt % organoclay, the peak corresponding to the interlayer spacing of the 5 wt % is shifted from $2\theta = 3.44$ to 2.8 (31 \AA) and this is due to the intercalation of organoclay by PP. But the intensity of the peak remains strong indicating that clay platelets are not well exfoliated. However, for the Gelimat-mixed nanocomposites with 5 wt % organoclay, the peak intensity almost completely disappeared and this can be attributed to the exfoliation and excellent dispersion of clay platelets in the PP matrix.

TEM

Figure 3 shows TEM images of Gelimat-mixed and extruded nanocomposites with 5 and 3 wt % organo-

clay. Images clearly indicate that the clay in Gelimat-mixed nanocomposites is exfoliated to a greater extent than for the extruded nanocomposites. Clay tactoids are smaller, less dense, and better dispersed in the Gelimat-mixed nanocomposites (images on the left) than for the extruded nanocomposites (images on the right). Those results are consistent with the XRD patterns shown in Figure 2.

Melt viscosity

Figure 4 shows the complex viscosity of the pure PP, the extruded nanocomposites and the Gelimat-mixed nanocomposites. The viscosity of nanocomposites at high frequency is similar to that of PP. The viscosity of nanocomposites prepared with both the Gelimat and the extruder is increased in the low-frequency region but in different magnitude. The complex viscosity of

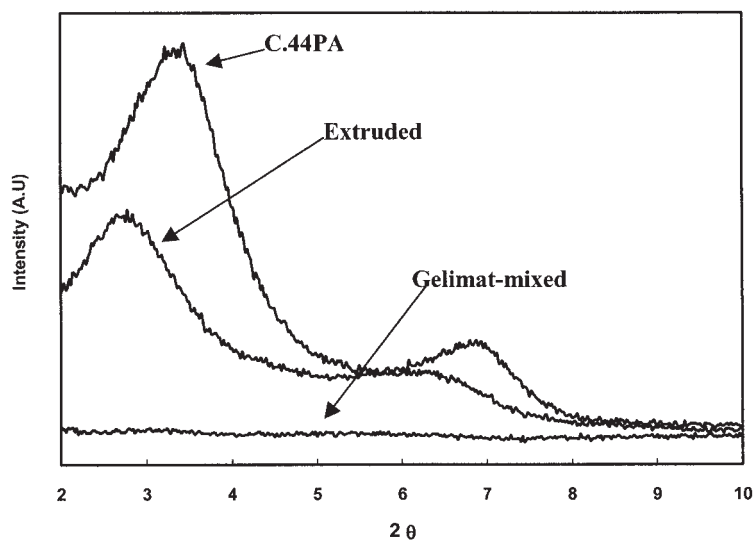


Figure 2 X-ray diffraction patterns of C.44PA, extruded, and Gelimat-mixed nanocomposites containing 5 wt % organoclay.

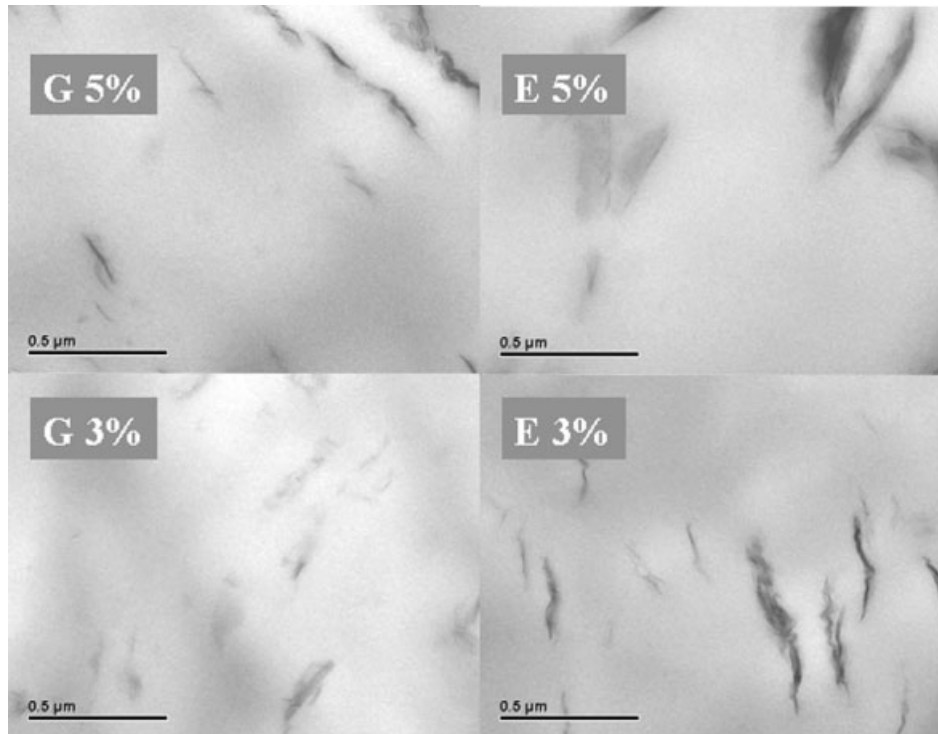


Figure 3 TEM images of Gelimat-mixed (G) and extruded (E) nanocomposites containing 5 and 3 wt % organoclay.

the Gelimat-mixed nanocomposites is higher than that of the corresponding extruded ones. This increase in viscosity of nanocomposites can be attributed to better clay dispersion within the PP matrix. This polymer clay interaction increases with the extent of exfoliated structure and this causes an increase in the viscosity of the nanocomposites. This observation is consistent with previous studies.^{3,5,12}

Tensile properties

In Figure 5, the modulus of 0, 3, and 5 wt % of PP/clay nanocomposites produced with a Gelimat and a twin-screw extruder was compared. The modulus of nanocomposites produced by both techniques increases with clay content but in different magnitude. The nanocomposites produced by the Gelimat exhibits

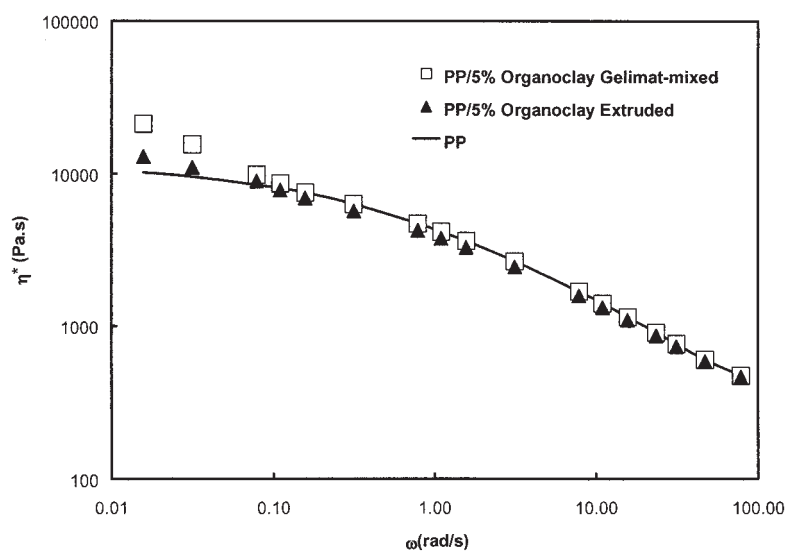


Figure 4 Complex viscosity (η^*) measured at 170°C as a function of the angular frequency (ω) for PP, extruded, and Gelimat-mixed nanocomposites containing 5 wt % organoclay.

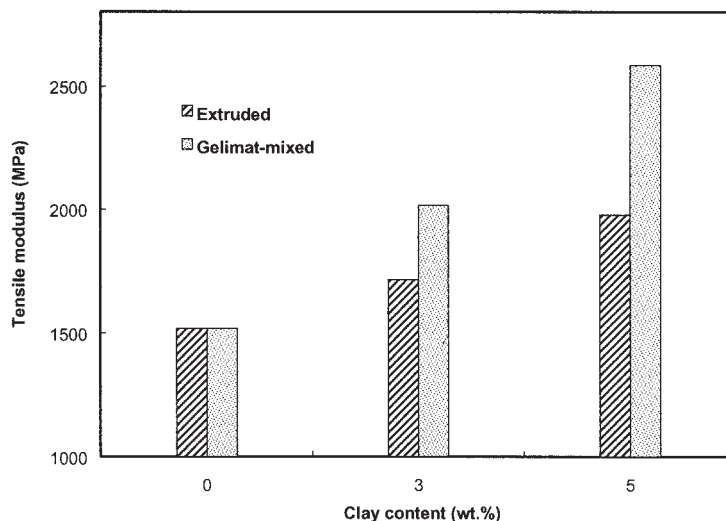


Figure 5 Tensile moduli of PP, extruded, and Gelimat-mixed nanocomposites (SD ± 70 MPa).

higher modulus than that prepared by extrusion, which can be attributed to a better exfoliation of the clay platelets. This observation is consistent with the XRD and TEM results. The tensile strength results shown in Figure 6 are less significant but show a similar trend between nanocomposites produced by extrusion as well as the Gelimat. Last, the strain at yield is reported in Figure 7 and shows a marked decrease for the nanocomposites. The strain at break was also measured but results fell within a standard deviation between Gelimat-mixed and extruded nanocomposites. Strain at break for PP and the nanocomposites was, respectively, 600–700 and 200–300%. These tensile property results show similar trends to previous work studying materials with comparable compositions.¹³ The mechanical properties of the PP/

clay nanocomposites have shown to be particularly sensitive to the amount, the chemical structure, and the molecular weight of the compatibilizer.^{13,14}

Shear rate calculations

Slow-motion photography of the Gelimat mixing chamber⁹ near the end of the compounding process has revealed that the material coagulates upon melting and accumulates on the edge and tip of the blade. In addition, the authors of this work have found some material stuck to the walls of the mixing chamber after some compounding runs. Those two observations led us to believe that the mixing action of the material in the melt state most likely occurs between the tip of the

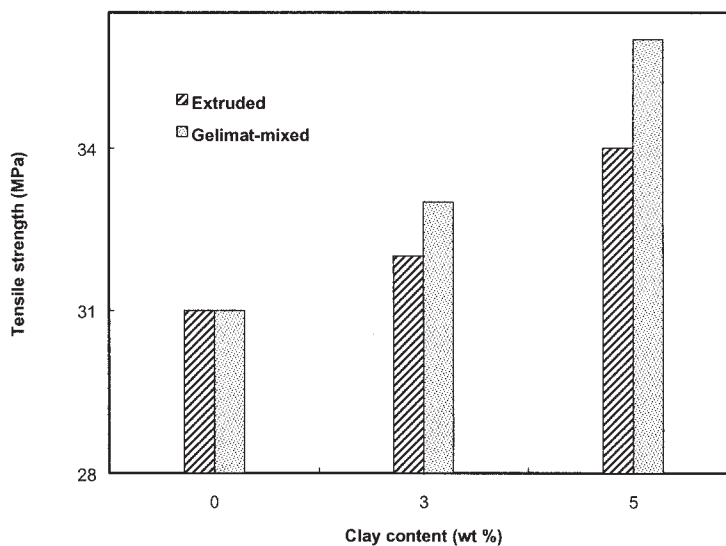


Figure 6 Tensile strengths of PP, extruded, and Gelimat-mixed nanocomposites. (std dev ± 2 MPa).

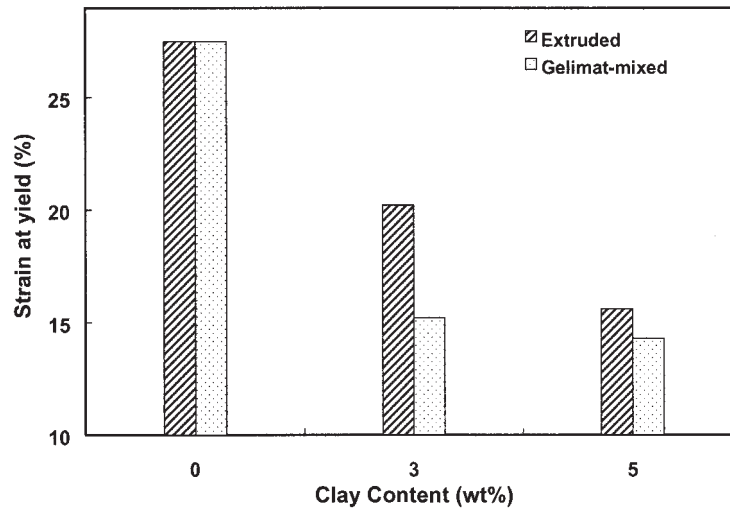


Figure 7 Strain at yield of PP, extruded, and Gelimat-mixed nanocomposites (SD \pm 2%).

blade and the wall due to the centrifugal forces produced by the rotating blade.

Calculations by the authors, made from the fluid properties, the dimensions of the Gelimat mixing chamber/shaft, and the rpm, indicate that shear rates around 10^4 s^{-1} can be generated between the tip of the blade and the chamber walls.

The non-Newtonian behavior of the polymer melts can be modeled using the power law defined in Eq. (1), where τ is the shear stress, $\dot{\gamma}$ is the shear rate, k is the fluid consistency, and n is the power law exponent.¹⁵

$$\tau = k\dot{\gamma}^n. \quad (1)$$

The shear stress generated between the tip of the rotating blade and the wall of the mixing chamber can be calculated from the dragging force F , which is given by the torque T divided by the radius r , and the shear area A , which is the product of the segment $r\theta$ covered by the thickness of the blade at the tip, and the length of the blade L . At any given radius between the blade and the wall, the shear stress can be calculated with Eq. (2)¹⁵ shown below.

$$\tau_r = \frac{T}{\theta r^2 L} \quad (2)$$

Using the above two equations, the shear rate at any given radius $\dot{\gamma}_r$ can be solved¹⁵ and expressed with Eq. (3). Figure 8 shows a schematic cross-sectional view of the Gelimat mixing chamber where Ω_b is the blade rotational velocity in radians per second, R_w is the radius at the wall, and R_b is the radius at the tip of the blade.

$$\dot{\gamma}_r = \frac{(2/n)\Omega_b r^{-2/n}}{(R_w^{-2/n} - R_b^{-2/n})} \quad (3)$$

Equation (3) is based on the laminar flow of a molten polymer and should be used only as a first approximation of the shear rate. This simplifying assumption neglects potential turbulence effects¹⁵ as a result of the fluid being pushed outward by centrifugal forces. Furthermore, the partially molten state of the polymer would result in much higher shear rates being applied on the liquid phase.

Shear rates developed in the Gelimat were estimated from the dimensions of the mixing chamber, the fluid shear thinning property, and Eq. (3). The power law exponent was calculated from the slope $(1 - n)$ of the viscosity linear region in Figure 3 to be $n = 0.5$. Where $R_w = 69 \text{ mm}$ and $R_b = 66 \text{ mm}$, the shear rates at the tip of the blade and at the wall were calculated to be, respectively, 5500 and 4600 s^{-1} at a blade speed of 2000 rpm . At 6000 rpm , those shear rates are, respectively, $16,400$ and $13,900 \text{ s}^{-1}$.

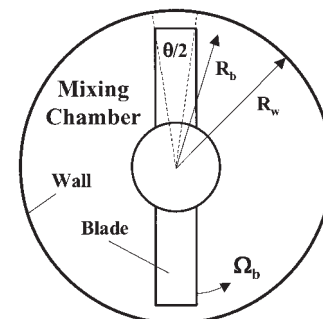


Figure 8 Schematic representation of the cross-sectional view of the Gelimat mixing chamber.

The delamination and dispersion of clay platelets within the studied polymer matrix was therefore attributed to the high shear stresses generated by the high-speed shaft of the Gelimat. Where extruders can typically generate shear rates in the range of 10^2 - 10^3 s^{-1} ¹⁵, shear rates about 10^4 s^{-1} were calculated for the Gelimat. This implies that the larger shear stresses induced during thermokinetic mixing are responsible for a better exfoliation. The difference in the structure and properties of the extruded nanocomposites may be due to insufficient mixing and thermal degradation of the organic intercalant from the organoclay.^{6,14}

CONCLUSIONS

PP/montmorillonite clay nanocomposites have been prepared by melt mixing PP with different levels of a predispersed organoclay masterbatch PP/clay concentrate. Melt mixing was achieved using a Gelimat, a high-speed thermokinetic mixer, and a corotating twin-screw extruder. The structure and properties of the nanocomposites prepared with the Gelimat were compared to ones produced with the twin-screw extruder. XRD and TEM results indicate that the Gelimat-mixed nanocomposites displayed a better exfoliation of the clay. Higher tensile modulus and strength were recorded for the Gelimat-mixed materials than for the extruded ones. The Gelimat was found to be a very effective tool for dispersing clay in a polymer matrix.

The authors thank the Center for Automotive Materials and Manufacturing in Kingston and Queen's Chemical Engineering department for the use of some of their equipment.

REFERENCES

1. Pinnavaia, T. J.; Beall, G. W., editors. *Polymer-Clay Nanocomposites*, Wiley: New York, 2001.
2. Kawasumi, M.; Hasegawa, N.; Kato, M.; Usuki, A.; Okada, A. *Macromolecules* 1997, 30, 6333.
3. Gopakumar, T. G.; Lee, J. A.; Kontopoulou, M.; Parent, J. S. *Polymer* 2002, 43, 5483.
4. Hambir, S.; Bulakh, N.; Kodgire, P.; Kalaonkar, R.; Jog, J. P. *J Appl Polym Sci* 2001, 39, 446.
5. Galgali, G.; Ramesh, C.; Lele, A. *Macromolecules* 2001, 34, 852.
6. Rong, M. Z.; Zhang, M. Q.; Zheng, Y. X.; Zeng, H. M.; Walter, R.; Friedrich, K. *Polymer* 2001, 42, 167.
7. Koo, C. M.; Kim, S. O.; Chung, I. J. *Macromolecules*, 2003, 36, 2748.
8. Busigin, C.; Lahtinen, R.; Martinez, G. M.; Thomas, G.; Woodhams, R. T. *Polym Eng Sci* 1984, 24, 169.
9. Baker, W.; Patel, P.; Catani, A. *Dynamics of a High Speed Melter/Mixer*; SPE ANTEC Proceedings, Paper 1986, 32, 1205.
10. Frenken, S.; Lyons, D.; Baker, W. E. *Slow Motion Filming and Predictive Modeling of a Gelimat K-Mixer*; SPE ANTEC Proceedings, 40, 1991.
11. Lyons, D.; Baker, W. E. *Intern Polym Process* 1990, V, 136.
12. Gopakumar, T. G.; Pagé, D. J. Y. S. *Polym Eng Sci* 2004, 44, 1162.
13. Svoboda, P.; Changchun, Z.; Wang, H.; Lee, L. J.; Tomasko, D. L. *J Appl Polym Sci* 2002, 85, 1562.
14. Ton-That, M.-T.; Cole, K. C.; Denault, J.; Perrin, F. *Polypropylene Nanocomposites: Formation and Performance*, International SAMPE Technical Conference, v 33 2001, p 720-727.
15. Rodriguez, F. *Principles of Polymer Systems*, 3rd ed., Hemisphere: New York, 1989.